Am J Cancer Res 2020;10(10):3230-3247
www.ajcr.us /ISSN:2156-6976/ajcr0117850

Original Article

Capsaicin acts through tNOX (ENOX2) to induce autophagic apoptosis in p53-mutated HSC-3 cells but autophagy in p53-functional SAS oral cancer cells

Chin-Fang Chang[1,2,3,4], Atikul Islam[5], Pei-Fen Liu[6], Jun-Han Zhan[7], Pin Ju Chueh[5,8,9]

[1]Department of Otolaryngology, Head and Neck Surgery, Jen-Ai Hospital, Taichung 41265, Taiwan; [2]Department of Medical Education and Research, Jen-Ai Hospital, Taichung 41265, Taiwan; [3]Cancer Medicine Center, Jen-Ai Hospital, Taichung 41265, Taiwan; [4]Basic Medical Education Center, Central Taiwan University of Science and Technology, Taichung 40601, Taiwan; [5]Institute of Biomedical Sciences, National Chung Hsing University, 145 Xingda Road, Taichung 40227, Taiwan; [6]Department of Food Science and Biotechnology, National Chung Hsing University, 145 Xingda Road, South District, Taichung 40227, Taiwan; [7]Bachelor Program of Biotechnology, National Chung Hsing University, 145 Xingda Road, Taichung 40227, Taiwan; [8]Department of Medical Research, China Medical University Hospital, Taichung 40402, Taiwan; [9]Graduate Institute of Basic Medicine, China Medical University, Taichung 40402, Taiwan

Received July 8, 2020; Accepted September 1, 2020; Epub October 1, 2020; Published October 15, 2020

Abstract: Despite the progress that has been made in diagnosing and treating oral cancers, they continue to have a poor prognosis, with a 5-year overall survival rate of approximately 50%. We have intensively studied the anticancer properties of capsaicin (a burning constituent of chili pepper), mainly focusing on its apoptotic properties. Here, we investigated the interplay between apoptosis and autophagy in capsaicin-treated oral cancer cells with either functional or mutant p53. Cytotoxicity was determined by cell impedance measurements and WST-1 assays, and cell death was analyzed by flow cytometry. The interaction between capsaicin and tumor-associated NADH oxidase (tNOX, ENOX2) was studied by cellular thermal shift assay (CETSA) and isothermal dose-response fingerprint curves ($ITDRF_{CETSA}$). Our CETSA data suggested that capsaicin directly engaged with tNOX, resulting in its degradation through the ubiquitin-proteasome and the autophagy-lysosome systems. In p53-functional SAS cells, capsaicin induced significant cytotoxicity via autophagy but not apoptosis. Given that tNOX catalyzes the oxidation of NADH, the direct binding of capsaicin to tNOX also inhibited the NAD^+-dependent activity of sirtuin 1 (SIRT1) deacetylase, we found that capsaicin-induced autophagy involved enhanced acetylation of ULK1, which is a key player in autophagy activation, possibly through SIRT1 inhibition. In p53-mutated HSC-3 cells, capsaicin triggered both autophagy and apoptosis. In this case, autophagy occurred before apoptosis: during this early stage, autophagy seemed to inhibit apoptosis; at a later stage, in contrast, autophagy appeared to be essential for the induction of apoptosis. Western blot analysis revealed that the reduction in tNOX and SIRT1 associated with enhanced ULK1 acetylation and c-Myc acetylation, which in turn, reactivated the TRAIL pathway, ultimately leading to apoptosis. Taken together, our data highlight the potential value of leveraging capsaicin and tNOX in therapeutic strategies against oral cancer.

Keywords: Apoptosis, autophagy, capsaicin, silent mating type information regulation 1 (Sirtuin 1, SIRT1), tumor-associated NADH oxidase (tNOX, ENOX2), oral cancer

Introduction

Autophagy and apoptosis are well-regulated cellular pathways that are often triggered in response to a wide variety of stress conditions; both ultimately govern the adjustment of cytoplasmic organelles or entire cells to maintain cellular homeostasis, although in most cases apoptosis represents a self-killing mechanism whereas autophagy is for self-protection [1-3]. Given that autophagy and apoptosis may be induced by common upstream signals and can occur in the same cell, the complex relationship between apoptosis and autophagy has been extensively discussed in the literature. Various related concepts have been introduced, such as sequential activation, inhibitory crosstalk, and autophagy-facilitated apoptosis [1, 3]. Th-

us, it is not surprising that the inhibition/activation of either apoptosis or autophagy affects the other process and can have many pathophysiological consequences.

Capsaicin (8-methyl-*N*-vanillyl-6-nonenamide) is a pungent component of chili peppers that has been long established to be a cancer-suppressing agent that shows apoptotic activity against numerous cancer cells lines [4-8]. Not surprisingly, growing evidence suggests that capsaicin also regulates autophagy, alone or more often in association with apoptosis. It has been shown that capsaicin activates endoplasmic reticulum transient receptor potential vanilloid receptor type I (TRPV1) to trigger both caspase-dependent apoptosis and autophagy in human osteosarcoma G292 cells, but that the latter signaling activates ERK to enhance cell survival [9]. In human hepatocellular carcinoma cells, suppression of capsaicin-triggered ROS-STAT3-dependent autophagy has been shown to augment capsaicin-induced apoptosis [10]. Conversely, exposure of human nasopharyngeal carcinoma cells to capsaicin was reported to attenuate PI3K/Akt/mTOR signaling to induce autophagy, which in turn activates caspase-3 and apoptosis [11]. These diverging cellular responses place capsaicin in the crucial position of funneling cells to either cell death or survival through the interplay of autophagy and apoptosis depending on cellular contexts.

Another desirable aspect of capsaicin is its preferential anticancer properties, which are evidenced by the fact that non-cancerous cells exhibit relatively higher tolerance for capsaicin [4, 12-15]. One explanation for this selective cytotoxicity resides in the growth-related NADH (or hydroquinone) oxidase (tNOX, ENOX2), which is universally expressed in cancer cells but not in non-transformed cells [4, 16-18]. tNOX was the first protein target to mechanistically link capsaicin to apoptosis and at least partly explain its preferential cytotoxicity in cancer cells [4]. Since then, numerous studies have addressed the involvement of tNOX in the impact of capsaicin on various cellular functions, such as cell cycle progression, migration/EMT, and apoptosis [19-25]. Interestingly, through inhibition on tNOX activity, capsaicin decreases the NAD^+/NADH ratio and the deacetylase activity of SIRT1 toward p53 acetylation to enhance cytotoxic apoptosis in cancerous A549 cells, whereas it triggers survival autophagy is non-cancerous MRC-5 cells, which lack tNOX expression [15]. However, it was previously unknown whether tNOX is involved in the cross-talk between apoptosis and autophagy in capsaicin-treated cells.

The cellular thermal shift assay (CETSA) identifies target proteins based on the principle that a target protein will unfold and precipitate, upon heating, whereas a protein engaged with a ligand will generally require a higher temperature to unfold and precipitate [26-31]. Here, we utilized CETSA and isothermal dose-response fingerprint curves to show that capsaicin directly binds to tNOX in oral cancer cells. The engagement between tNOX and capsaicin resulted in its protein degradation, which in turn triggered cytotoxic autophagy in p53-functional SAS cells. Interestingly, capsaicin mediated the sequential activation of both autophagy and apoptosis in p53-mutated HSC-3 cells, and the latter was found to be facilitated by the former. In both oral cancer cell lines, capsaicin treatment ultimately led to growth suppression, which is consistent with the idea that capsaicin has anticancer properties regardless of p53 functionality.

Materials and methods

Cell culture and reagents

Capsaicin (purity > 95%) was purchased from Sigma-Aldrich Corporation (St. Louis, MO, USA). The anti-SIRT1, anti-Atg5, anti-p53, anti-acetyl-p53, anti-phosphorylated mTOR, anti-mTOR, anti-ULK1, anti-PARP, anti-TRAIL, anti-Bak, anti-Bax, anti-PUMA, anti-Bcl2, anti-c-Flip, and anti-acetylated Lysine antibodies were purchased from Cell Signaling Technology, Inc. (Beverly, MA, USA). The anti-β-actin and anti-acetyl-c-Myc antibodies were from Millipore Corp. (Temecula, CA, USA). The anti-ubiquitin and anti-c-Myc antibodies were purchased from Santa Cruz Biotechnology, Inc. (Santa Cruz, CA, USA). The anti-p62 antibody was from BD Biosciences (San Jose, CA, USA). The anti-Beclin 1, anti-Atg7, and anti-LC3 antibodies were obtained from Novus biologicals (Centennial, CO, USA). The commercially available anti-COVA1 (a.k.a. tNOX, ENOX2) antibody from Proteintech (Rosemont, IL, USA) was used for immunoprecipitation. The antisera to tNOX used for immunoblotting were generated as described previously [32]. The anti-mouse and anti-rabbit IgG

antibodies and other chemicals were purchased from the Sigma Chemical Company (St. Louis, MO, USA), unless otherwise specified.

SAS (human squamous cell carcinoma of the tongue) and HSC-3 (human tongue squamous cell carcinoma) cells were grown in Dulbecco's Modified Eagle Medium (DMEM), were kindly provided by Dr. Yuen-Chun Li (Department of Biomedical Sciences, Chung Shan Medical University, Taiwan). Media were supplemented with 10% FBS, 100 units/ml penicillin and 50 μg/ml streptomycin. Cells were maintained at 37°C in a humidified atmosphere of 5% CO_2 in air, and the media were replaced every 2-3 days. Cells were treated with different concentrations of capsaicin (dissolved in ethanol), as described in the text, or with the same volume of ethanol (vehicle control).

Continuous monitoring of cell growth by cell impedance measurements

For continuous monitoring of changes in cell growth, cells (10^4 cells/well) were seeded onto E-plates and incubated for 30 min at room temperature, after which E-plates were placed onto the xCELLigence System (Roche, Mannhein, Germany). Cells were grown overnight before exposed to capsaicin or ethanol and impedance was measured every hour, as previously described [15]. Cell impedance is defined by the cell index (CI) = $(Z_i\text{-}Z_0)$ [Ohm]/15[Ohm], where Z_0 is background resistance and Z_i is the resistance at an individual time point. A normalized cell index was determined as the cell index at a certain time point (CI_{ti}) divided by the cell index at the normalization time point (CI_{nml_time}).

WST-1 cell viability assay

Cells (5×10^3) were seeded in 96-well culture plates and permitted to adhere overnight at 37°C in medium containing 10% serum. Cells were then treated with different concentrations of capsaicin for 24, 48 hours, and at the end of treatment, cell viability was determined using a WST-1 assay (Roche Applied Science, Mannheim, Germany) as described by the manufacturer. All experiments were performed at least in triplicate on three independent experiments.

Apoptosis determination

Apoptosis was measured using an Annexin V-FITC Apoptosis Detection Kit (BD Pharmingen, San Jose, CA, USA). Cells cultured in 6-cm dishes were trypsinized and collected by centrifugation. The cell pellet was washed, resuspended in 1x binding buffer and stained with annexin V-FITC (fluorescein isothiocyanate), as recommended by the manufacturer. Cells were also stained with propidium iodide (PI) to detect necrosis or late apoptosis. The distribution of viable (FITC/PI double-negative), early apoptotic (FITC-positive), late apoptotic (FITC/PI double-positive) and necrotic (PI-positive/FITC-negative) cells was analyzed using a Beckman Coulter FC500 flow cytometer. The results are expressed as a percentage of total cells.

Autophagy determination

Autophagosomes-acidic intracellular compartments that mediate the degradation of cytoplasmic materials during autophagy-were visualized by staining with Acridine Orange (AO; Sigma Chemical Co.). After incubation, cells were washed with PBS and stained with 2 mg/ml AO for 10 min at 37°C. AO-stained cells were then washed, trypsinized, and analyzed using a Beckman Coulter FC500. The results are expressed as a percentage of total cells.

Reverse transcriptase-polymerase chain reaction (RT-PCR)

Total RNA from oral cancer cells was isolated using the TRIzol reagent (Gibco, Carlsbad, CA, USA). First strand cDNA was synthesized from 1 μg of total RNA using Superscript II (Life Technologies, Rockville, MD, USA). The following primers sets were used for PCR amplifications: tNOX, 5'-GAAGTGTGATGCCGATAACAG-3' (sense) and 5'-AGTACTAGAGCCCAGGCGAA-3' (antisense) and β-actin, 5'-ACTCACCTTGGTGGTGCATA-3' (sense) and 5'-ACACCTTGATGGGAAAGGTGG-3' (antisense). The reaction conditions consisted of 30 cycles of 95°C for 30 sec, 55°C for 30 sec, and 72°C for 1 min, followed by a final extension of 5 min at 72°C. The obtained PCR products were resolved by 1.4% agarose gels electrophoresis and visualized by ethidium bromide staining.

Measurement of reactive oxygen species (ROS)

Oxidative stress was determined by measuring the level of hydrogen peroxide (H_2O_2) generated in the cells, as assessed by 5-(6)-carboxy-2',7'-

dichlorodihydrofluorescein diacetate (carboxy-H_2DCFDA) staining. The nonpolar, nonionic H_2-DCFDA is cell permeable and is hydrolyzed to nonfluorescent H_2-DCF by intracellular esterases. In the presence of peroxide, H_2-DCF is rapidly oxidized to highly fluorescent DCF. In brief, at the end of test compound treatment, cells (2×10^5) were washed with PBS and incubated with 5 μM H_2DCFDA in binding buffer for 30 min. The cells were then collected by trypsinization and centrifugation, washed with PBS, centrifuged at 200×g for 5 min and analyzed immediately using a Beckman Coulter FC500 flow cytometer.

SIRT1 activity measurement

The cellular SIRT1 activity was measured using a SIRT1 Activity Assay Kit (Fluorometric)(Abcam Inc. Cambridge, MA, USA). Briefly, 1×10^5 cells (either untreated or capsaicin-treated for 24 h) were washed, harvested and resuspended in 1 mL of lysis buffer (10 mM Tris-HCl pH 7.5, 10 mM NaCl, 15 mM $MgCl_2$, 250 mM sucrose, 0.5% NP-40, 0.1 mM EGTA). Cell lysates were sonicated 4 times for 5 seconds each on ice, and were centrifuged for 20 min at 4°C. The supernatant was then used for the determination of SIRT1 activity according to the manufacturer's instructions.

Cellular target identification of capsaicin by cellular thermal shift assay (CETSA)

Intracellular tNOX as cellular target of capsaicin was established by CETSA. Samples were prepared from control and capsaicin-exposed cells. For each set, 2×10^7 cells were seeded in a 10-cm cultured dish. After 24 h of culture, the cells were pretreated with 10 μM MG132 for 1 h, washed with PBS, treated with trypsin, and collected. Samples were centrifuged at 12,000 rpm for 3 min at room temperature, the pellets were gently resuspended with 1 mL of PBS, and the samples were centrifuged at 7,500 rpm for 3 min at room temperature. The pellets were resuspended with 1 mL of PBS containing 20 mM Tris-HCl pH 7.4, 100 mM NaCl, 5 mM EDTA, 2 mM phenylmethylsulfonyl fluoride (PMSF), 10 ng/ml leupeptin, and 10 μg/ml aprotinin. The samples were transferred to Eppendorf tubes and subjected to three freeze-thaw cycles; for each cycle, they were exposed to liquid nitrogen for 3 min, placed in a heating block at 37°C for 3 min, and vortexed briefly. For the experimental sample set, capsaicin was added to a final concentration of 2 mM; for the control sample set, the same volume of vesicle solvent was added. The samples were heated at 37°C for 1 h and dispensed to 100 μl aliquots. Pairs consisting of one control aliquot and one experimental aliquot were heated at 40°C, 43°C, 46°C, 49°C, 52°C, 55°C, 58°C, or 61°C for 3 min. Insoluble proteins were separated by centrifugation at 12,000 rpm for 30 min at 4°C, and the supernatants with soluble proteins were used for SDS-PAGE and Western blot analysis using antisera to tNOX [32, 33]. β-actin was used as the control.

The procedure for establishing an isothermal dose-response fingerprint ($ITDRF_{CETSA}$) was similar to that of the CETSA melting curve experiments as described above. Cells were seeded in 60 mm cultured dishes. After 24 h of culture, the cells were pretreated with 10 μM MG132 and exposed to different final concentrations of 0.001, 0.01, 0.05, 0.5, 1, 10, 50, 100, 200 μM capsaicin for 1 h, washed with PBS, treated with trypsin, and collected with centrifugation at 12,000 rpm for 2 min at room temperature. The pellets were gently resuspended with 1 mL of PBS, and then centrifuged at 7,500 rpm for 3 min at room temperature, and resuspended with PBS containing 20 mM Tris-HCl pH 7.4, 100 mM NaCl, 5 mM EDTA, 2 mM phenylmethylsulfonyl fluoride (PMSF), 10 ng/ml leupeptin, and 10 μg/ml aprotinin, and then subjected to three freeze-thaw cycles; for each cycle, they were exposed to liquid nitrogen for 3 min, placed in a heating block at 25°C for 3 min, and vortexed briefly. The samples were then heated at 54°C for 3 min and cooled for 3 min at room temperature. Insoluble proteins were separated by centrifugation at 12,000 rpm for 30 min at 4°C, and the supernatants with soluble proteins were used for SDS-PAGE and Western blot analysis using antisera to tNOX. β-actin was used as the control.

Immunoblotting and immunoprecipitation

Cell extracts were prepared in lysis buffer (20 mM Tris-HCl pH 7.4, 100 mM NaCl, 5 mM EDTA, 2 mM phenylmethylsulfonyl fluoride (PMSF), 10 ng/ml leupeptin, 10 μg/ml aprotinin). Volumes of extract containing equal amounts of proteins (40 μg) were applied to SDS-PAGE gels, and

resolved proteins were transferred to PVDF membranes (Schleicher & Schuell, Keene, NH, USA). The membranes were blocked, washed, and probed with primary antibody. After washing to remove unbound primary antibody, membranes were incubated with horseradish peroxidase-conjugated secondary antibody for one hour. The blots were washed again and developed using enhanced chemiluminescence (ECL) reagents, according to the manufacturer's protocol (Amersham Biosciences, Piscataway, NJ, USA).

For immunoprecipitation, protein extracts from 100 mm dishes were incubated with 30 µl of Protein G Agarose Beads (for rabbit antibodies) for 1 h at 4°C in rotation for pre-clearing. ENOX2/ULK1 antibodies or control IgG were incubated onto beads in 500 µl of PBS-Tween 20 1% for overnight in rotation at 4°C. Beads were precipitated by centrifugation at 3000 rpm, 2 min at 4°C and 80 µl of supernatants were collected for input total lysates. Beads were washed five times with lysis buffer and samples were prepared for Western blotting analysis.

Statistics

All data are expressed as the means ± SEs of three independent experiments. The significance of differences between control and treatment groups was calculated using a one-way ANOVA.

Results

CETSA melt and ITDRF$_{CETSA}$ curves indicate that capsaicin interacts with intracellular tNOX

To verify that capsaicin interacts with intracellular tNOX in oral cancer cells, we used CETSA to monitor the cellular target interaction based on that their direct binding enhances the thermal stability of a target protein in intact cells [27, 28]. We plotted the relative intensity of the tNOX signal against the temperature to generate CETSA curves, and used these curves to calculate melting temperatures (T_m; the temperature at which 50% of proteins are unfolded and rapidly precipitated by heat). A marked difference was observed in the curves of controls compared to capsaicin-treated lysates of both SAS cells (**Figure 1A**) and HSC-3 cells (**Figure 1B**). Upon capsaicin treatments, the T_m increased from 44.1 to 50.6°C in SAS cells and 44.6 to 51.2°C in HSC-3 cells, indicating that capsaicin triggered thermal stabilization of tNOX through direct binding. We also tested the dose-response relationship between capsaicin and the heat stability of tNOX. The dose-response study was conducted at 54°C, as a major portion of tNOX was denatured and precipitated at this temperature unless it was thermally stabilized by capsaicin. We observed that the stability of tNOX dose-dependently increased with the amount of applied capsaicin, with OC_{50} values of 46 and 44 µM for SAS cells (**Figure 1C**) and HSC-3 cells (**Figure 1D**), respectively. These data suggest that capsaicin directly interacts with intracellular tNOX.

Capsaicin mediates tNOX downregulation through ubiquitin-proteasomal and autophagy-lysosomal degradation

We next assessed the changes in tNOX expression upon its binding to capsaicin. Although multiple lines of evidence indicate that tNOX is down-regulated by capsaicin [15, 19, 21-25], the details of the underlying molecular mechanisms are not yet fully understood. Here, we used a cycloheximide-chase assay to verify that 200 µM capsaicin significantly attenuated the stability of tNOX, and found that this effect was seen starting at 6 h in SAS cells and at 12 h in HSC-3 cells (**Figure 2A**). Pre-treatment with the proteasome inhibitor, MG132, significantly restored the stability of tNOX following exposure to capsaicin in both oral cancer cells lines (**Figure 2B**), indicating that proteasomal degradation was involved in the ability of capsaicin to reduce tNOX expression. Similarly, we found that chloroquine, the lysosome inhibitor, marked reversed capsaicin-mediated tNOX down-regulation in both lines, suggesting that tNOX was also degraded through the autophagy-lysosome system (**Figure 2C**). Immunoprecipitation experiments performed with a commercially available antibody against endogenous tNOX and immunoblotting with anti-ubiquitin antibody, showed that tNOX was ubiquitinated in SAS cells and that, as expected, the ubiquitin levels of tNOX were enhanced in capsaicin-exposed cells compared to controls (**Figure 2D**). Capsaicin was also found to inhibit the transcriptional level of tNOX; this was observed at 100 and 200 µM for SAS cells and at 200 µM for HSC-3 cells (**Figure 2E**).

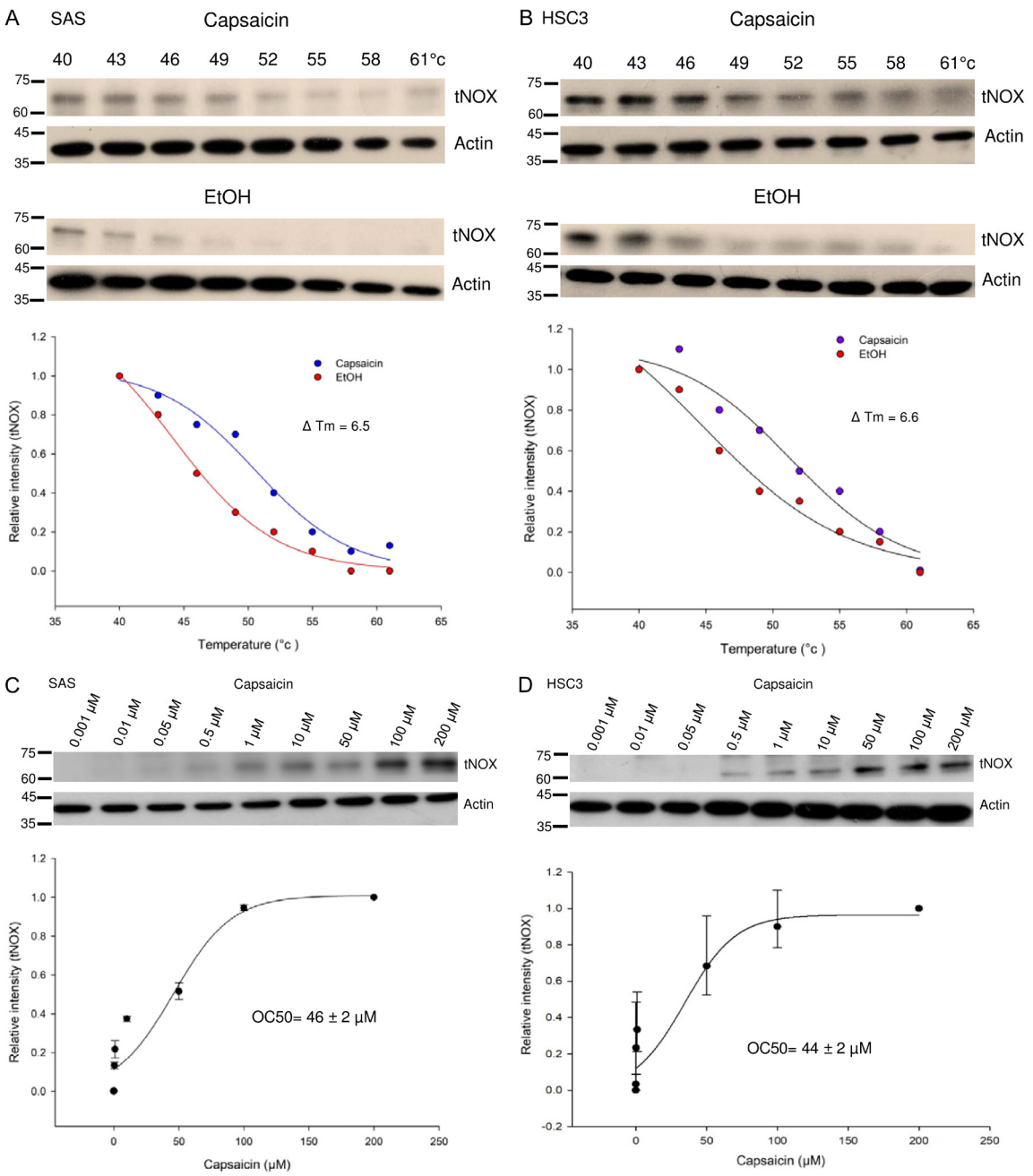

Figure 1. CETSA-based determination of binding between capsaicin and tNOX protein. (A, B) CETSA-melting curves of tNOX in the presence and absence of capsaicin as described in the Material and Methods in SAS cells (A) and HSC-3 cells (B). The immunoblot intensity was normalized to the intensity of the 40°C sample. Representative images are shown. The denaturation midpoints were determined using a standard process. (C, D) Cells were incubated with different concentrations of capsaicin as described in the Material and Methods. Dose dependent thermal stabilization of tNOX was assessed after heating samples at 54°C for 3 min in SAS cells (C) and HSC-3 cells (D). The band intensities of tNOX were normalized with respect to the intensity of actin. Representative images are shown.

Capsaicin preferentially induces cytotoxic autophagy, but not apoptosis, in SAS cells

We next examined the cellular consequences of the capsaicin-suppression of tNOX expression. To determine whether capsaicin induced differential effect in the tested cell lines, we continuously monitored the dynamic effects of capsaicin on cell growth by measuring cell impedance, and displayed the results as cell

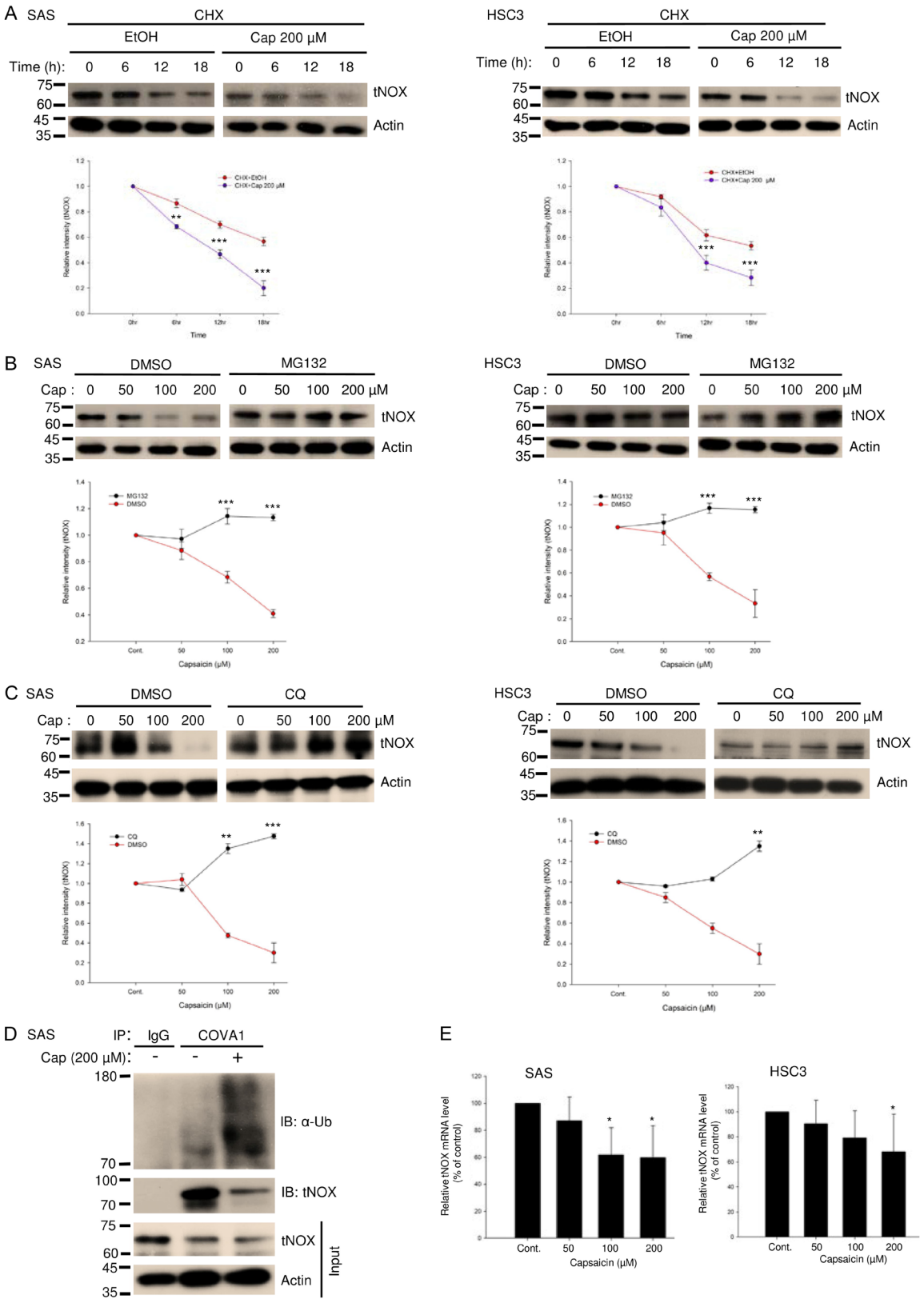

Figure 2. Capsaicin-induced tNOX downregulation is associated with ubiquitin-proteasomal and autophagy-lysosomal degradation. A. Capsaicin (200 μM) markedly attenuated tNOX stability as assessed with a cycloheximide-chase assay in a time-dependent manner in SAS cells and HSC-3 cells. B. Capsaicin-induced tNOX downregulation was reverted by MG132, the proteasome inhibitor, in SAS cells and HSC-3 cells. C. Capsaicin-induced tNOX downregula-

tion was reverted by CQ, the lysosome inhibitor, in SAS cells and HSC-3 cells. Aliquots of cell lysates were separated by SDS-PAGE and analyzed by Western blotting. β-Actin was detected as an internal control. Representative images are shown. Values (mean ± S. E.) are from at least three independent experiments (*P < 0.05, ***P < 0.001 for capsaicin-treated cells vs. controls). D. SAS cells were treated with 200 μM capsaicin or ethanol for 24 h. The cell lysates were immunoprecipitated with nonimmune IgG or a commercially available anti-COVA1 antibody against endogenous tNOX, and the bound proteins were detected by Western blotting with ubiquitin or tNOX antibodies. E. Cells were exposed to capsaicin or ethanol and the RNA levels of tNOX were analyzed by RT-PCR.

index (CI) values [34-37]. This approach revealed that capsaicin repressed the growth of SAS and HSC-3 cells; it showed comparable levels of cytotoxicity in the two cell lines (**Figure 3A**). Similar results were obtained with a cell viability assay, indicating that capsaicin induced dose- and time-dependent decreases in the cell viability of these oral cancer cell lines (**Figure 3B**).

Mutations in p53 contribute to most cancers, but relatively little work has examined the antineoplastic properties of capsaicin against cells with mutated p53. Here, we used human oral squamous cell carcinoma-derived SAS and HSC-3 cells, which differ in their p53 functionality. In SAS cells, p53 has an early stop codon that generates a truncated protein, but the phosphorylation on key residue S46 preserves its apoptotic function according to the mutation list found on the TP53 website (http://p53.free.fr/Database/Cancer_cell_lines/p53_cell_lines.html). Interestingly, capsaicin (100 and 200 μM) induced autophagy (**Figure 4A**), not apoptosis (**Figure 4B**), in SAS cells. Pretreatment with the autophagy inhibitor 3-methyladenine (3-MA) and lysosome inhibitor chloroquine (CQ) significantly enhanced both spontaneous and capsaicin-induced apoptosis in these cells (**Figure 4C**), suggesting that capsaicin-mediated autophagy is inhibitory to apoptosis in our experimental system. Given that tNOX inhibition/tNOX knockdown is associated with reduces intracellular NAD^+ generation and SIRT1 inhibition [15, 19, 38-40], we evaluated the expression of SIRT1 in our system. In cells treated with 100 or 200 μM of capsaicin, the expression levels of tNOX and SIRT1 were concurrently attenuated; those of beclin-1, Atg5 (autophagy-related 5), Atg7, p62, and cleaved LC3 II were increased; and that of p-mTOR (mechanistic target of rapamycin) was decreased (**Figure 4D**). All of these findings indicated that autophagy was induced in capsaicin-exposed SAS cells. The capsaicin-induced suppression of SIRT1 was accompanied by a decrease in the SIRT1-unc-51 like autophagy activating kinase 1 (ULK1) interaction by immunoprecipitation with an antibody against ULK1 and immunoblotting with anti-SIRT1 antibody (**Figure 4E**). The capsaicin-enhanced acetylation of ULK1 was also validated by immunoprecipitation, which is another key regulator of autophagy (**Figure 4F**). Interestingly, the acetylation of p53 was not markedly enhanced by capsaicin; this might explain the deficit of apoptosis in these cells, which was also evidenced by a lack of PARP cleavage (**Figure 4D**). We did not observe any notable generation of reactive oxygen species (ROS), suggesting that ROS might not be a major signaling pathway for capsaicin-mediated autophagy in SAS cells (**Figure 4G**).

Capsaicin induces autophagic apoptosis in HSC-3 cells

We also studied the cellular outcomes in capsaicin-exposed HSC-3 cells, which fail to phosphorylate p53 at Ser46, show defective transcriptional activation of proapoptotic genes, and are resistant to apoptosis [41, 42]. Interestingly, our results demonstrated that capsaicin at 200 μM noticeably triggered both apoptosis and autophagy in HSC-3 cells (**Figure 5A**). Given this, we sought to dissect the interplay between autophagy and apoptosis in these cells. In time-dependent experiments, we found that autophagy preceded apoptosis (**Figure 5B**). Pretreatment with the autophagy inhibitor 3-MA and lysosome inhibitor CQ, seemed to increase capsaicin-induced apoptosis at 12 h exposure (**Figure 5C**). This suggested that there was a sequential activation of autophagy and apoptosis, and that early-stage autophagy inhibited apoptosis. In contrast, blockage of autophagy evidently repressed capsaicin-induced apoptosis at 18 or 24 h exposure (**Figure 5D**), suggesting that autophagy-facilitated apoptosis occurred if the stress continued long enough. However, ROS signaling seemed to play a minor role in capsaicin-mediated cell death in this system (**Figure 5E**).

Based on the Western blot analysis, protein expression levels of tNOX and SIRT1 were inhib-

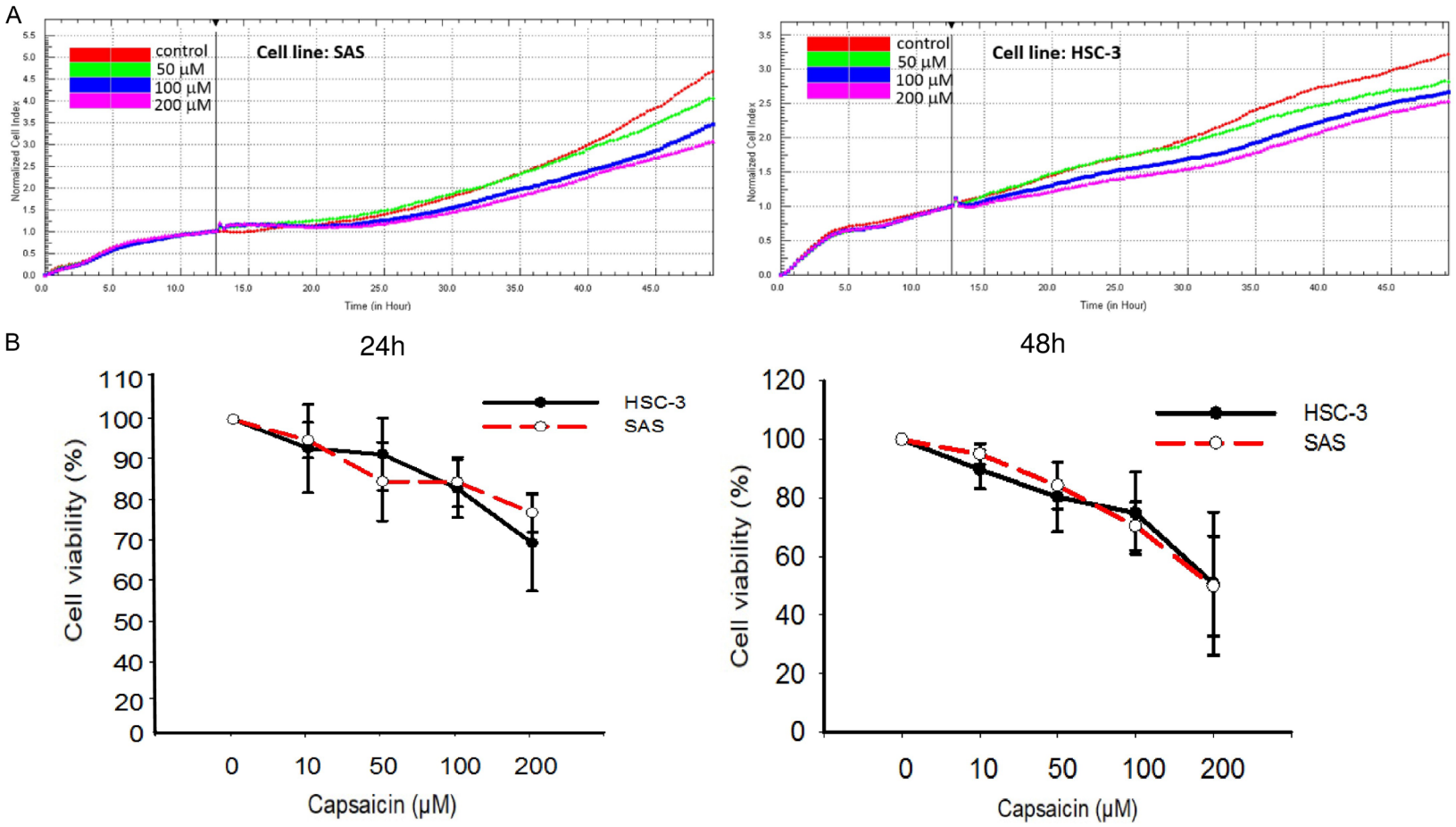

Figure 3. Capsaicin represses oral cancer cell growth. A. Dynamic monitoring of cell proliferation was performed using impedance technology, as described in the Materials and Methods section. Normalized cell index values measured over 50 h are shown. B. Cells were exposed to different concentrations of capsaicin for 24 or 48 h and cell viability was measured using WST assays. Values (means ± SDs) are from three independent experiments.

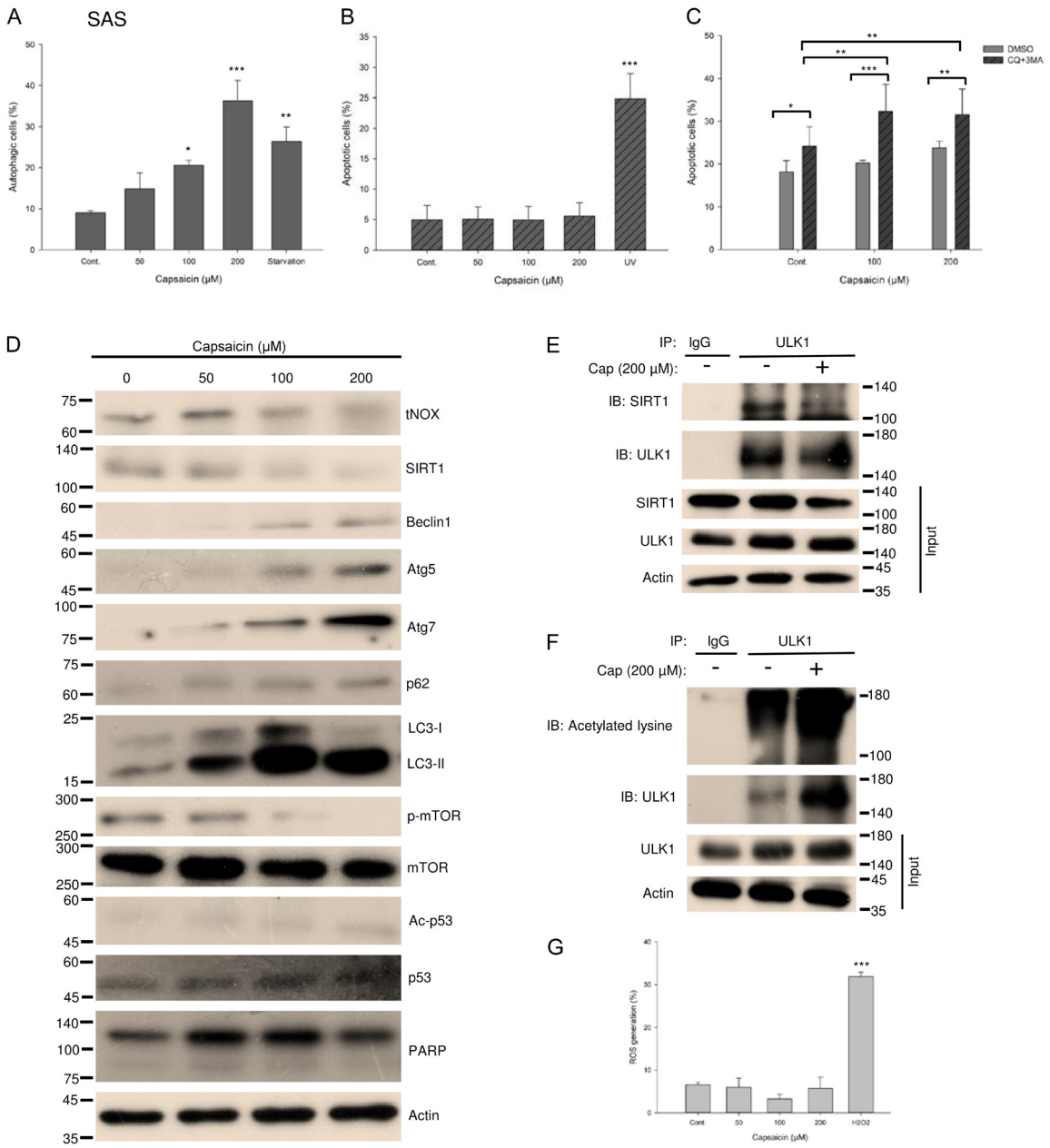

Figure 4. Capsaicin preferentially induces autophagy but not apoptosis in SAS cells. A. SAS cells were treated with capsaicin or ethanol for 15 hours. Autophagy was determined by AO staining using flow cytometry, analysis and the results are expressed as a percentage of autophagic cells. Values (mean ± S. E.) are from at least three independent experiments (**P* < 0.05, ***P* < 0.01, ****P* < 0.001). B. Cells were treated with capsaicin or ethanol for 24 hours. The percentage of apoptotic cells was determined by flow-cytometry, and the results are presented as the percentage of apoptotic cells. Values (mean ± S. E.) are from at least three independent experiments (****P* < 0.001). C. Cells were pretreated with or without 10 μM 3-MA and 25 μM CQ for 1 h before exposure to capsaicin or ethanol for 24 hours. The percentage of apoptotic cells was assessed by flow cytometry, and the results are expressed as a percentage of apoptotic cells. Values (mean ± S. E.) are from at least three independent experiments (**P* < 0.05, ***P* < 0.01, ****P* < 0.001). D. SAS cells were treated with capsaicin or ethanol for 24 hours. Aliquots of cell lysates were separated by SDS-PAGE and analyzed for protein expression by Western blotting; β-actin was used as an internal control to monitor for equal loading. Representative images are shown from at least two independent experiments. E, F. The lysates of SAS cells were immunoprecipitated with nonimmune IgG or an antibody against pan-acetylated lysine, and the bound proteins were detected by Western blotting with ULK1 or pan-acetylated lysine antibodies. G. The percent change in intracellular ROS generation was measured after cells were exposed to different concentrations of capsaicin for 1 h.

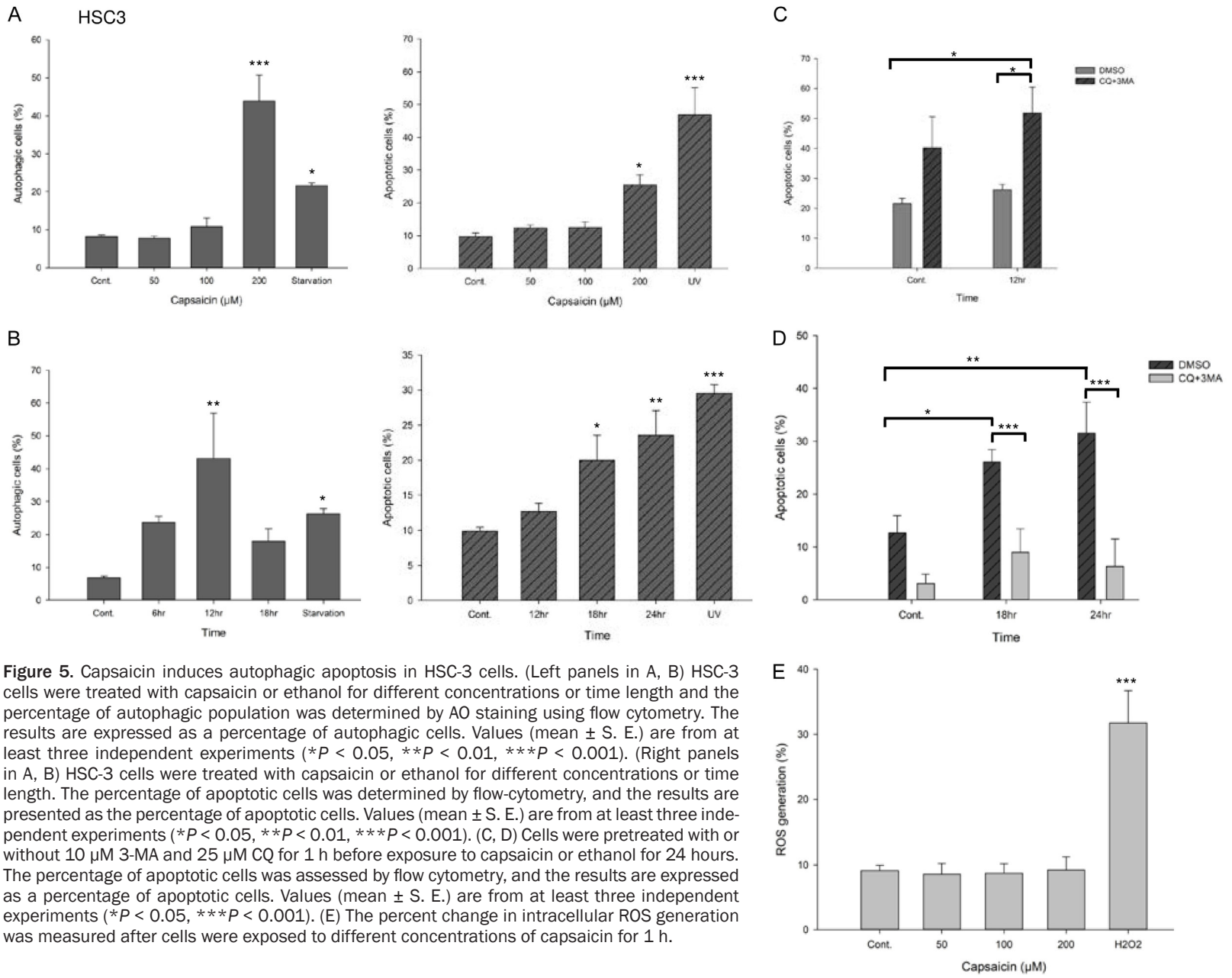

Figure 5. Capsaicin induces autophagic apoptosis in HSC-3 cells. (Left panels in A, B) HSC-3 cells were treated with capsaicin or ethanol for different concentrations or time length and the percentage of autophagic population was determined by AO staining using flow cytometry. The results are expressed as a percentage of autophagic cells. Values (mean ± S. E.) are from at least three independent experiments (*P < 0.05, **P < 0.01, ***P < 0.001). (Right panels in A, B) HSC-3 cells were treated with capsaicin or ethanol for different concentrations or time length. The percentage of apoptotic cells was determined by flow-cytometry, and the results are presented as the percentage of apoptotic cells. Values (mean ± S. E.) are from at least three independent experiments (*P < 0.05, **P < 0.01, ***P < 0.001). (C, D) Cells were pretreated with or without 10 μM 3-MA and 25 μM CQ for 1 h before exposure to capsaicin or ethanol for 24 hours. The percentage of apoptotic cells was assessed by flow cytometry, and the results are expressed as a percentage of apoptotic cells. Values (mean ± S. E.) are from at least three independent experiments (*P < 0.05, ***P < 0.001). (E) The percent change in intracellular ROS generation was measured after cells were exposed to different concentrations of capsaicin for 1 h.

ited by 200 μM of capsaicin, and this was accompanied by downregulation of phosphorylated-mTOR, and up-regulation of Beclin 1 and cleaved PARP, demonstrating the induction of autophagy and apoptosis (**Figure 6A**). Our time-dependent experiments showed that tNOX and SIRT1 were inhibited at 12 h, and this was accompanied by up-regulation of Atg 7, Atg5, p62, beclin 1, and LC3 cleavage at 12 h of exposure (**Figure 6B**). Capsaicin at 200 μM significantly inhibited cellular SIRT1 deacetylase activity in HSC-3 cells using a SIRT1 activity assay kit (**Figure 6C**). Due to the suppression of cellular SIRT1 activity and possible tNOX-SIRT1 axis, we observed an enhancement of ULK1 acetylation (**Figure 6D**). Moreover, several apoptosis markers, such as acetylated c-Myc, TRAIL, Bak, Bax, cleaved caspase-3, PUMA, and cleaved PARP, were enhanced at 18 and 24 h of exposure to capsaicin (**Figure 6E**). Anti-apoptotic proteins, such as C-Flip and Bcl-2, were attenuated at 18 and 24 h of exposure to capsaicin (**Figure 6E**). These data further confirm that capsaicin treatment of HSC-3 triggered autophagy at an early stage, and that this autophagy subsequently fostered the induction of apoptosis. Blockade of autophagy up to 12 h seemed to promote capsaicin-induced apoptosis (**Figure 5C**), whereas a later blockade of autophagy interfered with apoptosis in these cells (**Figure 5D**).

Discussion

Oral cancers, which belong to the head and neck cancer groups, include cancers of the lining of the lips, mouth, and upper throat. The updated database, GLOBOCAN, estimated that there were 355,000 new diagnoses of oral cancers and over 177,000 oral cancer-related deaths worldwide in 2018 [43]. Although a large body of research has sought to refine the diagnosis and treatment of oral cancer, the prognosis of oral cancer patients has not significantly improved, and the 5-year overall survival is approximately 50% [44]. The tumor suppressor, p53, is mutated in various types of solid malignancies, including head and neck cancers, and p53 mutations hugely impact the treatment resistance, progression, and recurrence of these cancers [45-48]. However, whether p53 mutations affect the anticancer properties of capsaicin has not been fully addressed. Our present results demonstrated that capsaicin suppresses growth of human oral squamous carcinoma cells regardless of their p53 status through targeting tNOX; more precisely, capsaicin induced cytotoxic autophagy in SAS cells (with functional p53), while inducing both autophagy and apoptosis in p53-mutated HSC-3 cells (**Figure 7**). Reports from other groups have shown that capsaicin possesses antiproliferative activity and could induce apoptosis in p53-wild-type, p53-null, and p53-mutant prostate cancer cells [49, 50]. A more recent report found that capsaicin eliminated mutated p53 through autophagic degradation and reactivated wild-type p53 transcriptional activity to induce lung cancer cell death [51]. These lines of evidence, together with our present results, emphasize that capsaicin has immense scope as an anticancer regimen to induce cell death irrespective of the cellular p53 status.

Apoptosis remains the most prominent anticancer property of capsaicin, but emerging data suggest that autophagy is also involved in the complex mechanisms through which capsaicin acts against cancer. Autophagy can be cytoprotective or cytotoxic and is often intertwined with apoptosis, and the mechanisms underlying capsaicin-induced autophagy are likely to be complex. In most cases, capsaicin-induced autophagy is a pro-survival and/or anti-apoptotic process [9, 10, 52-56]. However, some studies have found that capsaicin can provoke a cytotoxic autophagy that coexists or cooperates with apoptosis to accelerate cell death [11, 52]. In this present study, a relatively simple scenario was observed in SAS cells, where capsaicin induced autophagy alone and caused irreversible destruction, leading to cellular demise and growth attenuation. However, a more complex crosstalk between autophagy and apoptosis was observed in HSC-3 cells. In the latter cell line, autophagy was developed as a primary response, reflecting the instinct of the cell to adapt to capsaicin when exposure did not exceed a critical duration. Upon a longer exposure that presumably exceeded some threshold, however, the cells executed an autophagy-facilitated form of apoptosis. Thus, capsaicin-treated HSC-3 cells exhibited sequential activation of both autophagy and apoptosis.

One compelling finding of this study is that tNOX-SIRT1 appears to form a regulatory axis in the capsaicin-induced autophagy and apoptosis of oral cancer cells. The association bet-

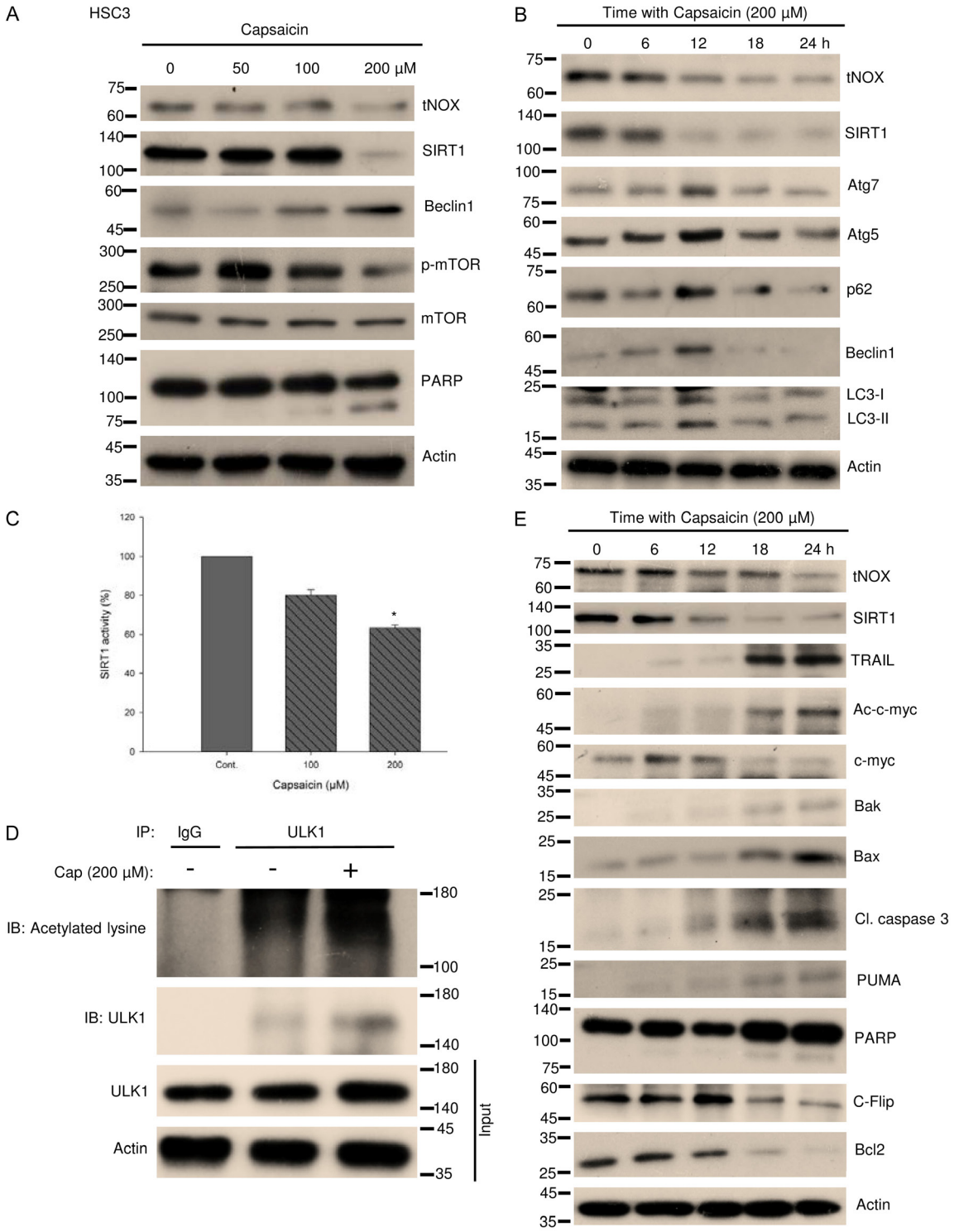

Figure 6. Capsaicin induces autophagy at an early stage and subsequent apoptosis in HSC-3 cells. A, B, E. HSC-3 cells were treated with capsaicin or ethanol for different concentrations or time length. Aliquots of cell lysates were separated by SDS-PAGE and analyzed for protein expression by Western blotting; β-actin was used as an internal control to monitor for equal loading. Representative images are shown from at least two independent experiments. C. Capsaicin-inhibited cellular SIRT1 activity was determined using a SIRT1 Activity Assay Kit (Fluorometric) with control or capsaicin-treated HSC-3 cell lysates. Values (mean ± S. E.) are from three independent experiments (*P < 0.05, ***P < 0.001). D. The lysates of HSC-3 cell were immunoprecipitated with nonimmune IgG or an antibody against pan-acetylated lysine, and the bound proteins were detected by Western blotting with ULK1 or pan-acetylated lysine antibodies.

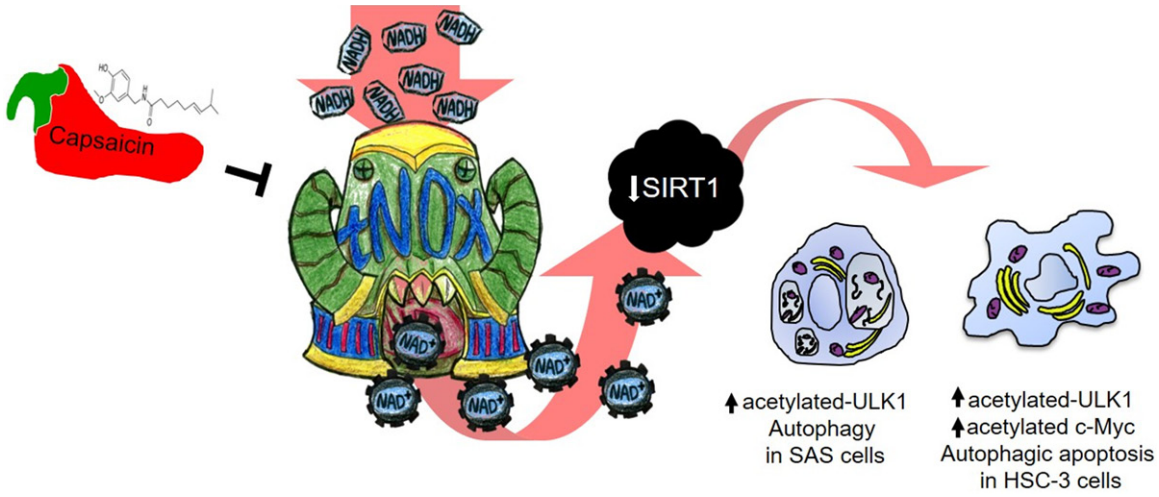

Figure 7. Schematic diagram of the mechanism governing capsaicin-induced cytotoxic autophagy in SAS p53 functional oral cancer cells and autophagic apoptosis in HSC-3 p53 mutated oral cancer cells.

ween tNOX inhibition and capsaicin-induced apoptosis has long been recognized in cancer/transformed cells [4, 23-25]. Most recently, we added to this knowledge base by showing that capsaicin suppresses the tNOX-NAD^+-SIRT1 axis to induce apoptosis through augmented p53 acetylation in A549 lung cancer cells [15]. SIRT1, which is the most widely studied member of the sirtuin family of NAD^+-dependent deacetylases, has received much attention for its predominant role in energy homeostasis and aging [57-59]. To date, relatively few studies have examined the correlation between capsaicin and SIRT1. For example, capsaicin was reported to enhance the acetylation of FOXO-1 to trigger apoptosis through modulation of SIRT deacetylase activity in a pancreatic tumor system [60]. In another study, capsaicin was found to exert protective effects by up-regulating SIRT1 in cardiomyocytes [61]. Similarly, we reported that capsaicin stimulates SIRT1 activity and induces cytoprotective autophagy in non-cancer MRC-5 cells, which lack tNOX expression [15]. We believe that the differential effects of capsaicin on SIRT1 expression and activity are associated with the presence of tNOX protein. In fact, our previous study has reported that capsaicin stimulated SIRT1 activity *in vitro*; however, depending on tNOX level, capsaicin induces opposing effects on SIRT1 activity *in vivo* as well as their subsequent cellular outcomes in cancer and non-cancer cells [15]. Continued accumulation of relevant knowledge is critically needed if we hope to exploit pathways involving tNOX or SIRT1 as legitimate targets for capsaicin-mediated cellular consequences. Indeed, we recently showed that ability of capsaicin to restrict the tNOX-NAD^+-SIRT1 axis retards cell cycle progression by enhancing the acetylation of c-Myc to restrain the G1 cyclin/CDK complex [22]. In another study, we reported that capsaicin inhibits SIRT1 to enhance the acetylation of cortactin and b-catenin, thereby decreasing the activation of MMP-2 and MMP-9 and eventually inhibiting the migration of bladder cancer cells [62]. Here, we add to this exciting body of knowledge by describing how the regulatory tNOX-NAD^+-SIRT1 axis contributes to capsaicin-induced cell death. More specifically, we show that capsaicin enhanced ULK1 acetylation to trigger autophagy in SAS cells, whereas it induces HSC-3 cells to first undergo autophagy and then, via a switch involving the increased acetylation of ULK1, undertake apoptosis through elevated acetylation of c-Myc and up-regulation of TRAIL (**Figure 7**).

Conclusions

Taken together, our identification of tNOX as a direct target of capsaicin and our elucidation of the involvement of the tNOX-NAD^+-SIRT1 regulatory axis provide insight into the molecular events underlying capsaicin-induced autophagy and apoptosis. Moreover, we herein show for the first time that the complex capsaicin-induced crosstalk between autophagy and

apoptosis relies on ULK1 and c-Myc. Finally, we provide evidence supporting the idea that the repressive effect of capsaicin on cancer cells is independent of p53 functionality. These findings collectively contribute to our ability to decipher the biological functions of capsaicin and provide a solid basis for understanding its chemopreventive activity.

Acknowledgements

The authors thank Dr. Show-Mei Chuang for the assistance in cell viability determination and Mr. Chia-An Yeh for his artistic drawing of tNOX function. This work was supported by grants from the Jen-Ai Hospital (to CFC) and the Ministry of Sciences and Technology, Taiwan (NSC 102-2320-B-005-008 to PJC).

Disclosure of conflict of interest

None.

Abbreviations

CETSA, Cellular thermal shift assay; ITDRF, Isothermal dose-response fingerprint; ROS, Reactive oxygen species; tNOX, tumor-associated NADH oxidase; SIRT1, Sirtuin 1.

Address correspondence to: Dr. Pin Ju Chueh, Institute of Biomedical Sciences, National Chung Hsing University, Taichung, Taiwan. Tel: +886 4 2284-0896; Fax: +886 4 22853469; E-mail: pjchueh@dragon.nchu.edu.tw

References

[1] Marino G, Niso-Santano M, Baehrecke EH and Kroemer G. Self-consumption: the interplay of autophagy and apoptosis. Nat Rev Mol Cell Biol 2014; 15: 81-94.

[2] Gordy C and He YW. The crosstalk between autophagy and apoptosis: where does this lead? Protein Cell 2012; 3: 17-27.

[3] Maiuri MC, Zalckvar E, Kimchi A and Kroemer G. Self-eating and self-killing: crosstalk between autophagy and apoptosis. Nat Rev Mol Cell Biol 2007; 8: 741-752.

[4] Morre DJ, Chueh PJ and Morre DM. Capsaicin inhibits preferentially the NADH oxidase and growth of transformed cells in culture. Proc Natl Acad Sci U S A 1995; 92: 1831-1835.

[5] Kim JD, Kim JM, Pyo JO, Kim SY, Kim BS, Yu R and Han IS. Capsaicin can alter the expression of tumor forming-related genes which might be followed by induction of apoptosis of a Korean stomach cancer cell line, SNU-1. Cancer Lett 1997; 120: 235-241.

[6] Gupta SC, Kim JH, Prasad S and Aggarwal BB. Regulation of survival, proliferation, invasion, angiogenesis, and metastasis of tumor cells through modulation of inflammatory pathways by nutraceuticals. Cancer Metastasis Rev 2010; 29: 405-434.

[7] Cho SC, Lee H and Choi BY. An updated review on molecular mechanisms underlying the anticancer effects of capsaicin. Food Sci Biotechnol 2017; 26: 1-13.

[8] Zhang SP, Wang DA, Huang JY, Hu YM and Xu YF. Application of capsaicin as a potential new therapeutic drug in human cancers. J Clin Pharm Ther 2020; 45: 16-28.

[9] Chien CS, Ma KH, Lee HS, Liu PS, Li YH, Huang YS and Chueh SH. Dual effect of capsaicin on cell death in human osteosarcoma G292 cells. Eur J Pharmacol 2013; 718: 350-360.

[10] Chen X, Tan M, Xie Z, Feng B, Zhao Z, Yang K, Hu C, Liao N, Wang T, Chen D, Xie F and Tang C. Inhibiting ROS-STAT3-dependent autophagy enhanced capsaicin-induced apoptosis in human hepatocellular carcinoma cells. Free Radic Res 2016; 50: 744-755.

[11] Lin YT, Wang HC, Hsu YC, Cho CL, Yang MY and Chien CY. Capsaicin induces autophagy and apoptosis in human nasopharyngeal carcinoma cells by downregulating the PI3K/AKT/mTOR pathway. Int J Mol Sci 2017; 18: 1343.

[12] Macho A, Calzado MA, Munoz-Blanco J, Gomez-Diaz C, Gajate C, Mollinedo F, Navas P and Munoz E. Selective induction of apoptosis by capsaicin in transformed cells: the role of reactive oxygen species and calcium. Cell Death Differ 1999; 6: 155-165.

[13] Kang HJ, Soh Y, Kim MS, Lee EJ, Surh YJ, Kim HR, Kim SH and Moon A. Roles of JNK-1 and p38 in selective induction of apoptosis by capsaicin in ras-transformed human breast epithelial cells. Int J Cancer 2003; 103: 475-482.

[14] Bley K, Boorman G, Mohammad B, McKenzie D and Babbar S. A comprehensive review of the carcinogenic and anticarcinogenic potential of capsaicin. Toxicol Pathol 2012; 40: 847-873.

[15] Lee YH, Chen HY, Su LJ and Chueh PJ. Sirtuin 1 (SIRT1) deacetylase activity and NAD(+)/NADH ratio are imperative for capsaicin-mediated programmed cell death. J Agric Food Chem 2015; 63: 7361-7370.

[16] Bruno M, Brightman AO, Lawrence J, Werderitsh D, Morré DM and Morré DJ. Stimulation of NADH oxidase activity from rat liver plasma membranes by growth factors and hormones is decreased or absent with hepatoma plasma membranes. Biochem J 1992; 284: 625-628.

[17] Chueh PJ. Cell membrane redox systems and transformation. Antioxid Redox Signal 2000; 2: 177-187.
[18] Chueh PJ, Wu LY, Morre DM and Morre DJ. tNOX is both necessary and sufficient as a cellular target for the anticancer actions of capsaicin and the green tea catechin (-)-epigallocatechin-3-gallate. Biofactors 2004; 20: 235-249.
[19] Lin MH, Lee YH, Cheng HL, Chen HY, Jhuang FH and Chueh PJ. Capsaicin inhibits multiple bladder cancer cell phenotypes by inhibiting tumor-associated NADH oxidase (tNOX) and sirtuin1 (SIRT1). Molecules 2016; 21: 849.
[20] Liu NC, Hsieh PF, Hsieh MK, Zeng ZM, Cheng HL, Liao JW and Chueh PJ. Capsaicin-mediated tNOX (ENOX2) up-regulation enhances cell proliferation and migration in vitro and in vivo. J Agric Food Chem 2012; 60: 2758-2765.
[21] Chen HY, Lee YH, Chen HY, Yeh CA, Chueh PJ and Lin YM. Capsaicin inhibited aggressive phenotypes through downregulation of tumor-associated NADH oxidase (tNOX) by POU domain transcription factor POU3F2. Molecules 2016; 21: 733.
[22] Islam A, Su AJ, Zeng ZM, Chueh PJ and Lin MH. Capsaicin targets tNOX (ENOX2) to inhibit G1 Cyclin/CDK complex, as assessed by the cellular thermal shift assay (CETSA). Cells 2019; 8: 1275.
[23] Mao LC, Wang HM, Lin YY, Chang TK, Hsin YH and Chueh PJ. Stress-induced down-regulation of tumor-associated NADH oxidase during apoptosis in transformed cells. FEBS Lett 2008; 582: 3445-3450.
[24] Wang HM, Chueh PJ, Chang SP, Yang CL and Shao KN. Effect of Ccapsaicin on tNOX (ENOX2) protein expression in stomach cancer cells. Biofactors 2008; 34: 209-217.
[25] Wang HM, Chuang SM, Su YC, Li YH and Chueh PJ. Down-regulation of tumor-associated NADH oxidase, tNOX (ENOX2), enhances capsaicin-induced inhibition of gastric cancer cell growth. Cell Biochem Biophys 2011; 61: 355-366.
[26] Dziekan JM, Wirjanata G, Dai L, Go KD, Yu H, Lim YT, Chen L, Wang LC, Puspita B, Prabhu N, Sobota RM, Nordlund P and Bozdech Z. Cellular thermal shift assay for the identification of drug-target interactions in the Plasmodium falciparum proteome. Nat Protoc 2020; 15: 1881-1921.
[27] Martinez Molina D, Jafari R, Ignatushchenko M, Seki T, Larsson EA, Dan C, Sreekumar L, Cao Y and Nordlund P. Monitoring drug target engagement in cells and tissues using the cellular thermal shift assay. Science 2013; 341: 84-87.
[28] Martinez Molina D and Nordlund P. The cellular thermal shift assay: a novel biophysical assay for in situ drug target engagement and mechanistic biomarker studies. Annu Rev Pharmacol Toxicol 2016; 56: 141-161.
[29] Simon GM, Niphakis MJ and Cravatt BF. Determining target engagement in living systems. Nat Chem Biol 2013; 9: 200-205.
[30] Lim YT, Prabhu N, Dai L, Go KD, Chen D, Sreekumar L, Egeblad L, Eriksson S, Chen L, Veerappan S, Teo HL, Tan CSH, Lengqvist J, Larsson A, Sobota RM and Nordlund P. An efficient proteome-wide strategy for discovery and characterization of cellular nucleotide-protein interactions. PLoS One 2018; 13: e0208273.
[31] Prabhu N, Dai L and Nordlund P. CETSA in integrated proteomics studies of cellular processes. Curr Opin Chem Biol 2020; 54: 54-62.
[32] Chen CF, Huang S, Liu SC and Chueh PJ. Effect of polyclonal antisera to recombinant tNOX protein on the growth of transformed cells. Biofactors 2006; 28: 119-133.
[33] Liu SC, Yang JJ, Shao KN and Chueh PJ. RNA interference targeting tNOX attenuates cell migration via a mechanism that involves membrane association of Rac. Biochem Biophys Res Commun 2008; 365: 672-677.
[34] Ke N, Wang X, Xu X and Abassi YA. The xCELLigence system for real-time and label-free monitoring of cell viability. Methods Mol Biol 2011; 740: 33-43.
[35] Moela P, Choene MM and Motadi LR. Silencing RBBP6 (Retinoblastoma Binding Protein 6) sensitises breast cancer cells MCF7 to staurosporine and camptothecin-induced cell death. Immunobiology 2014; 219: 593-601.
[36] Kuo YF, Su YZ, Tseng YH, Wang SY, Wang HM and Chueh PJ. Flavokawain B, a novel chalcone from alpinia pricei hayata with potent apoptotic activity: involvement of ROS and GADD153 upstream of mitochondria-dependent apoptosis in HCT116 cells. Free Radic Biol Med 2010; 49: 214-226.
[37] Su YC, Lin YH, Zeng ZM, Shao KN and Chueh PJ. Chemotherapeutic agents enhance cell migration and epithelial-to-mesenchymal transition through transient up-regulation of tNOX (ENOX2) protein. Biochim Biophys Acta 2012; 1820: 1744-1752.
[38] Tikhomirov AS, Shchekotikhin AE, Lee YH, Chen YA, Yeh CA, Tatarskiy VV Jr, Dezhenkova LG, Glazunova VA, Balzarini J, Shtil AA, Preobrazhenskaya MN and Chueh PJ. Synthesis and characterization of 4,11-Diaminoanthra[2,3-b]furan-5,10-diones: tumor cell apoptosis through tNOX-modulated NAD(+)/NADH ratio and SIRT1. J Med Chem 2015; 58: 9522-9534.
[39] Chen HY, Cheng HL, Lee YH, Yuan TM, Chen SW, Lin YY and Chueh PJ. Tumor-associated NADH oxidase (tNOX)-NAD+-sirtuin 1 axis contributes to oxaliplatin-induced apoptosis of

gastric cancer cells. Oncotarget 2017; 8: 15338-15348.
[40] Lin CY, Islam A, Su CJ, Tikhomirov AS, Shchekotikhin AE, Chuang SM, Chueh PJ and Chen YL. Engagement with tNOX (ENOX2) to inhibit SIRT1 and activate p53-dependent and -independent apoptotic pathways by novel 4,11-diaminoanthra[2,3-b]furan-5,10-diones in hepatocellular carcinoma cells. Cancers (Basel) 2019; 11: 420.
[41] Ichwan SJ, Yamada S, Sumrejkanchanakij P, Ibrahim-Auerkari E, Eto K and Ikeda MA. Defect in serine 46 phosphorylation of p53 contributes to acquisition of p53 resistance in oral squamous cell carcinoma cells. Oncogene 2006; 25: 1216-1224.
[42] Sakai E and Tsuchida N. Most human squamous cell carcinomas in the oral cavity contain mutated p53 tumor-suppressor genes. Oncogene 1992; 7: 927-933.
[43] Bray F, Ferlay J, Soerjomataram I, Siegel RL, Torre LA and Jemal A. Global cancer statistics 2018: GLOBOCAN estimates of incidence and mortality worldwide for 36 cancers in 185 countries. CA Cancer J Clin 2018; 68: 394-424.
[44] Lacas B, Bourhis J, Overgaard J, Zhang Q, Gregoire V, Nankivell M, Zackrisson B, Szutkowski Z, Suwinski R, Poulsen M, O'Sullivan B, Corvo R, Laskar SG, Fallai C, Yamazaki H, Dobrowsky W, Cho KH, Beadle B, Langendijk JA, Viegas CMP, Hay J, Lotayef M, Parmar MKB, Auperin A, van Herpen C, Maingon P, Trotti AM, Grau C, Pignon JP and Blanchard P; MARCH Collaborative Group. Role of radiotherapy fractionation in head and neck cancers (MARCH): an updated meta-analysis. Lancet Oncol 2017; 18: 1221-1237.
[45] Nigro JM, Baker SJ, Preisinger AC, Jessup JM, Hostetter R, Cleary K, Bigner SH, Davidson N, Baylin S, Devilee P, et al. Mutations in the p53 gene occur in diverse human tumour types. Nature 1989; 342: 705-708.
[46] Somers KD, Merrick MA, Lopez ME, Incognito LS, Schechter GL and Casey G. Frequent p53 mutations in head and neck cancer. Cancer Res 1992; 52: 5997-6000.
[47] Zhou G, Liu ZY and Myers JN. TP53 mutations in head and neck squamous cell carcinoma and their impact on disease progression and treatment response. J Cell Biochem 2016; 117: 2682-2692.
[48] Gunn GB, Blanchard P, Garden AS, Zhu XR, Fuller CD, Mohamed AS, Morrison WH, Phan J, Beadle BM, Skinner HD, Sturgis EM, Kies MS, Hutcheson KA, Rosenthal DI, Mohan R, Gillin MT and Frank SJ. Clinical outcomes and patterns of disease recurrence after intensity modulated proton therapy for oropharyngeal squamous carcinoma. Int J Radiat Oncol Biol Phys 2016; 95: 360-367.
[49] Lin HK, Altuwaijri S, Lin WJ, Kan PY, Collins LL and Chang CS. Proteasome activity is required for androgen receptor transcriptional activity via regulation of androgen receptor nuclear translocation and interaction with coregulators in prostate cancer cells. J Biol Chem 2002; 277: 36570-36576.
[50] Mori A, Lehmann S, O'Kelly J, Kumagai T, Desmond JC, Pervan M, McBride WH, Kizaki M and Koeffler HP. Capsaicin, a component of red peppers, inhibits the growth of androgen-independent, p53 mutant prostate cancer cells. Cancer Res 2006; 66: 3222-3229.
[51] Garufi A, Pistritto G, Cirone M and D'Orazi G. Reactivation of mutant p53 by capsaicin, the major constituent of peppers. J Exp Clin Cancer Res 2016; 35: 136.
[52] Wang Y, Deng X, Yu C, Zhao G, Zhou J, Zhang G, Li M, Jiang D, Quan Z and Zhang Y. Synergistic inhibitory effects of capsaicin combined with cisplatin on human osteosarcoma in culture and in xenografts. J Exp Clin Cancer Res 2018; 37: 251.
[53] Yoon JH, Ahn SG, Lee BH, Jung SH and Oh SH. Role of autophagy in chemoresistance: regulation of the ATM-mediated DNA-damage signaling pathway through activation of DNA-PKcs and PARP-1. Biochem Pharmacol 2012; 83: 747-757.
[54] Choi CH, Jung YK and Oh SH. Autophagy induction by capsaicin in malignant human breast cells is modulated by p38 and extracellular signal-regulated mitogen-activated protein kinases and retards cell death by suppressing endoplasmic reticulum stress-mediated apoptosis. Mol Pharmacol 2010; 78: 114-125.
[55] Liu YP, Dong FX, Chai X, Zhu S, Zhang BL and Gao DS. Role of autophagy in capsaicin-induced apoptosis in U251 glioma cells. Cell Mol Neurobiol 2016; 36: 737-743.
[56] Amantini C, Morelli MB, Nabissi M, Cardinali C, Santoni M, Gismondi A and Santoni G. Capsaicin triggers autophagic cell survival which drives epithelial mesenchymal transition and chemoresistance in bladder cancer cells in an Hedgehog-dependent manner. Oncotarget 2016; 7: 50180-50194.
[57] Imai S, Armstrong CM, Kaeberlein M and Guarente L. Transcriptional silencing and longevity protein Sir2 is an NAD-dependent histone deacetylase. Nature 2000; 403: 795-800.
[58] Vaziri H, Dessain SK, Eagon EN, Imai SI, Frye RA, Pandita TK, Guarente L and Weinberg RA. hSIR2 (SIRT1) functions as an NAD-dependent p53 deacetylase. Cell 2001; 107: 149-159.
[59] Houtkooper RH, Pirinen E and Auwerx J. Sirtuins as regulators of metabolism and healthspan. Nat Rev Mol Cell Biol 2012; 13: 225-238.

[60] Pramanik KC, Fofaria NM, Gupta P and Srivastava SK. CBP-mediated FOXO-1 acetylation inhibits pancreatic tumor growth by targeting SirT. Mol Cancer Ther 2014; 13: 687-698.

[61] He H, Zhou Y, Huang J, Wu Z, Liao Z, Liu D, Yin D and He M. Capsaicin protects cardiomyocytes against anoxia/reoxygenation injury via preventing mitochondrial dysfunction mediated by SIRT1. Oxid Med Cell Longev 2017; 2017: 1035702.

[62] Islam A, Yang YT, Wu WH, Chueh PJ and Lin MH. Capsaicin attenuates cell migration via SIRT1 targeting and inhibition to enhance cortactin and beta-catenin acetylation in bladder cancer cells. Am J Cancer Res 2019; 9: 1172-1182.